The Astrophysical Journal Letters, 763:L3 (5pp), 2013 January 20 doi:10.1088/2041-8205/763/1/L3

THE *PLANCK* SUNYAEV–ZEL'DOVICH VERSUS THE X-RAY VIEW OF THE COMA CLUSTER

R. Fusco-Femiano[1], A. Lapi[2,3], and A. Cavaliere[2,4]
[1] IAPS-INAF, Via Fosso del Cavaliere, I-00133 Roma, Italy
[2] Dip. Fisica, Univ. "Tor Vergata," Via Ricerca Scientifica 1, I-00133 Roma, Italy
[3] SISSA, Via Bonomea 265, I-34136 Trieste, Italy
[4] INAF, Osservatorio Astronomico di Roma, via Frascati 33, I-00040 Monteporzio, Italy
Received 2012 September 14; accepted 2012 December 10; published 2012 December 21

ABSTRACT

The *Planck* collaboration has recently published precise and resolved measurements of the Sunyaev–Zel'dovich (SZ) effect in Abell 1656 (the Coma cluster of galaxies), thus directly gauging the electron pressure profile in the intracluster plasma. On the other hand, such a quantity may be also derived from combining the density and temperature provided by X-ray observations of the thermal bremsstrahlung radiation emitted by the plasma. We find a model-independent tension between the SZ and the X-ray pressure, with the SZ one being definitely lower by 15%–20%. We propose that such a challenging tension can be resolved in terms of an additional, non-thermal support to the gravitational equilibrium of the intracluster plasma. This can be straightforwardly included in our Supermodel, so as to fit in detail the *Planck* SZ profile while being consistent with the X-ray observables. Possible origins of the non-thermal component include cosmic-ray protons, ongoing turbulence, and relativistic electrons; given the existing observational constraints on the first two options, here we focus on the third. For this to be effective, we find that the electron population must include not only an energetic tail accelerated to $\gamma \gtrsim 10^3$ responsible for the Coma radiohalo, but also many more, lower energy electrons. The electron acceleration is to be started by merging events similar to those that provided the very high central entropy of the thermal intracluster plasma in Coma.

Key words: cosmic background radiation – galaxies: clusters: individual (Abell 1656) – X-rays: galaxies: clusters

Online-only material: color figures

1. INTRODUCTION

We are motivated by the recent, spatially resolved measurements with the *Planck* satellite by Ade et al. (2012) of the Sunyaev & Zel'dovich (1980, hereafter SZ) effect in Abell 1656, the very rich, nearby cluster in Coma Berenices at $z = 0.023$.

The thermal SZ effect describes how the temperature of crossing cosmic microwave background (CMB) photons is modulated by the Compton upscattering of the hot electrons in the intracluster plasma (ICP). Its strength is given by the Comptonization parameter $y \equiv (\sigma_T/m_e c^2) \int d\ell\, p_e(r)$ integrated along lines of sight across the cluster. It directly probes the electron thermal pressure $p_e \approx p\,(2+2X)/(3+5X) \geqslant 0.5\,p$, here written in terms of the ICP pressure p; with the cosmic hydrogen abundance $X \approx 0.76$, their ratio reads $p_e/p = 0.52$. Compared with previous observations including *Wilkinson Microwave Anisotropy Probe* (*WMAP*; see Komatsu et al. 2011 and references therein), the resolved *Planck* data improve the SZ probing of the cluster core and extend it into the outskirts, providing a handle to the complex astrophysical processes in the ICP to be discussed here.

On the other hand, the ICP pressure $p \approx nk_BT/\mu$ (with the mean molecular weight $\mu \approx 0.60$) may be also derived from combining the density n and temperature T provided by X-ray observations of the thermal bremsstrahlung radiation emitted by the plasma. The overall trend emerging from the *Planck* data is toward a *deficit* in the SZ relative to the X-ray pressure; see Ade et al. (2012). In detail, these authors used empirical formulae suggested by numerical simulations (see Nagai et al. 2007) and by X-ray analyses (see Arnaud et al. 2010) to fit the SZ data. These formulae provide a "universal" pressure profile for the whole cluster population, or a specific version for unrelaxed clusters. However, when applied to fit the precise *Planck* SZ data, these formulae perform inadequately, as discussed by Ade et al. (2012); specifically, the first version overshoots the data in the core, and both appreciably undershoot them in the outskirts, well beyond the quoted uncertainties. Aimed modifications of the parameter values in the fitting formulae, which include suppression of unphysical central divergencies, can improve the SZ fits at the cost of inconsistencies with the X-ray pressure. As discussed by the above authors, this is also the case with multiparametric fitting formulae of the type proposed by Vikhlinin et al. (2006) for the X-ray observables.

Thus we are stimulated to use an *orthogonal* approach, provided by the Supermodel (SM; Cavaliere et al. 2009); this yields a direct *link* between the X-ray and the SZ observables (see Lapi et al. 2012). We specify below how the SM is based on a physically motivated run of the entropy $k(r) \equiv k_BT(r)/n^{2/3}(r)$, which underlies the ICP support in the gravitational potential well provided by the cluster dark matter, to approach hydrostatic equilibrium.

The SM improves in a number of respects upon the classic isothermal β-model (Cavaliere & Fusco-Femiano 1976), adopted by Mohr et al. (1999) and Churazov et al. (2012) to closely describe the central X-ray brightness profile in Coma. In fact, the SM incorporates updated, weakly cusped distributions of the dark matter (see Lapi & Cavaliere 2009). It also accurately describes the central conditions in both cool and in non-cool core clusters such as Coma (see Molendi & Pizzolato 2001). Finally, it also describes the region beyond a few 10^2 kpc where T declines outward while n drops, so that the entropy gradually rises as shown by many X-ray data (e.g., Snowden et al. 2008; Cavagnolo et al. 2009; Pratt et al. 2010;

Walker et al. 2012), and as expected on basic astrophysical grounds.

2. THE SUPERMODEL VIEW

In fact, the spherically averaged entropy profile rises from a central level k_c into an outer ramp with slope a toward the virial boundary R, following the pattern (Voit 2005; Lapi et al. 2005):

$$k(r) = k_c + k_R\,(r/R)^a. \quad (1)$$

Specifically, a central baseline $k_c \sim 10^2$ keV cm^2 is produced during the early collapse and virialization of the cluster core; then the intergalactic gas is condensed to levels $n \sim 10^{-3}$ cm^{-3} in step with the general overdensities around 200 over the average background, while it is heated up to temperatures $k_B T \approx GM/10\,R \sim$ a few keV. These conditions imply thermal pressures $p \approx 2\,n\,k_B T$, of the order of a few 10^{-11} erg cm^{-3}. The baseline k_c may be subsequently lowered by radiative cooling or enhanced by active galactic nucleus (AGN) feedback (see Lapi et al. 2003; Fabian 2012) and deep, energetic mergers (see Markevitch & Vikhlinin 2007; McCarthy et al. 2007). These processes, respectively, produce current conditions of the cool core kind with $k_c \sim 10$ keV cm^2, or of the non-cool core kind with $k_c > 10^2$ keV cm^2 like in Coma (Cavaliere et al. 2011).

At the outer end, the slope $a \approx 1$ and the boundary value $k_R \sim$ several 10^3 keV cm^2 are originated as entropy is continuously produced by strong virial accretion shocks (for observational evidence in Coma, see Brown & Rudnick 2011; Markevitch 2012), and then is conserved and stratified as the infalling gas is compressed into the gravitational potential well (Tozzi & Norman 2001; Cavaliere et al. 2011).

The SM formalism simply consists of inserting the entropy run of Equation (1) in the differential equation for hydrostatic equilibrium of the ICP (see Cavaliere et al. 2009 for details); this is easily integrated to obtain *linked* runs of the thermal pressure,

$$\frac{p(r)}{p_R} = \left[1 + \frac{2\,G\,m_p}{5\,p_R^{2/5}} \int_r^R dx \frac{M(<x)}{x^2\,k^{3/5}(x)}\right]^{5/2}, \quad (2)$$

of the density $n(r) \propto [p(r)/k(r)]^{3/5}$ and of the temperature $T(r) \propto p^{2/5}(r)\,k^{3/5}(r)$. Here, p_R is the value at the virial boundary, while $M(<r)$ is the gravitational mass distribution mainly contributed by the dark matter (see Lapi & Cavaliere 2009).

In Figure 1 we show how the SM fits the projected profiles of X-ray brightness $S_X \propto n^2\,T^{1/2}$ found by Churazov et al. (2012), and of the emission-weighted temperature T measured by Snowden et al. (2008) and Wik et al. (2009) in Coma; see Fusco-Femiano et al. (2009) for details. From these fits we extract values (with their 1σ uncertainty, and consistent with the last reference) of the parameters $k_c \approx 535 \pm 180$ keV cm^2, $a \approx 1.3 \pm 0.2$, and $k_R \approx 5050 \pm 225$ keV cm^2 specifying the entropy pattern in Equation (1).

Based on such values, Coma turns out to be an *extreme* HE (high entropy) cluster both in the *core* and in the *outskirts*, according to the classification used in Cavaliere et al. (2011). As discussed there, such conditions call for impacts of several energetic mergers down to the center that deposit energies of the order of 10^{64} ergs, and for strong accretion shocks standing at the virial boundary with Mach numbers $\mathcal{M} \sim 10$ that produce outer temperatures $k_B T_R \sim 5$ keV. Both processes are in tune with the rich, supercluster environment that surrounds Coma.

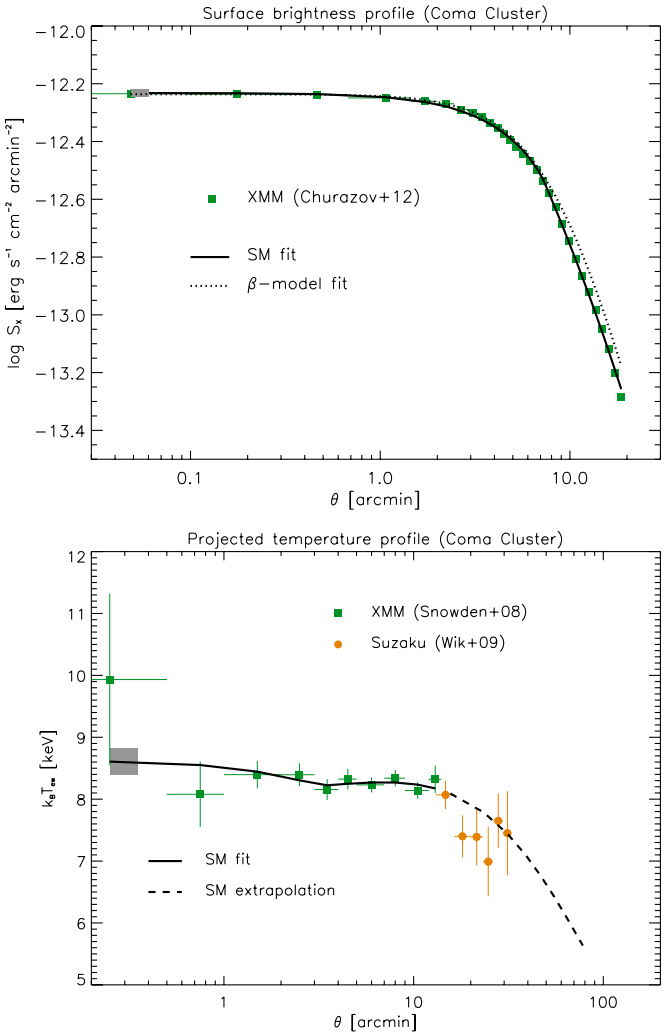

Figure 1. Top panel: profile of the X-ray surface brightness in the Coma cluster; the green squares refer to the *XMM-Newton* data by Churazov et al. (2012), the dotted line shows their β-model fit, while the solid line illustrates our SM outcome. Bottom panel: projected profile of the emission-weighted temperature in the Coma cluster; the green squares refer to the *XMM-Newton* data by Snowden et al. (2008), the orange circles to the *Suzaku* data by Wik et al. (2009), the solid line is our SM outcome (obtained on fitting the *XMM-Newton* data), with the dashed line representing its extrapolation into the outskirts out to the virial radius $R = 2.2$ Mpc (see Churazov et al. 2012). In both panels the shaded areas show the associated 2σ uncertainties.

(A color version of this figure is available in the online journal.)

From Equation (2) we find the radial pressure profile $p(r)$ with no recourse to delicate deprojections. Thence we obtain the *thermal* electron pressure p_e, and compute the profile of the corresponding SZ Comptonization parameter y (cf. Section 1). In Figure 2 we express our result in terms of the equivalent Rayleigh–Jeans decrement $\Delta T \equiv -2yT_{\rm CMB}$ of the CMB temperature $T_{\rm CMB} \approx 2.73$ K, to compare with the *Planck* measurements as presented by Ade et al. (2012), see their Figure 4.

3. COMPARING THE SZ AND X-RAY VIEWS OF COMA

Figure 2 highlights a *deficit* in the values of $|\Delta T|$ as measured by *Planck*, relative to those expected from the X-ray pressure. The discrepancy appears to be remarkably sharp at the center, well beyond the uncertainties budget presented by Ade et al. (2012).

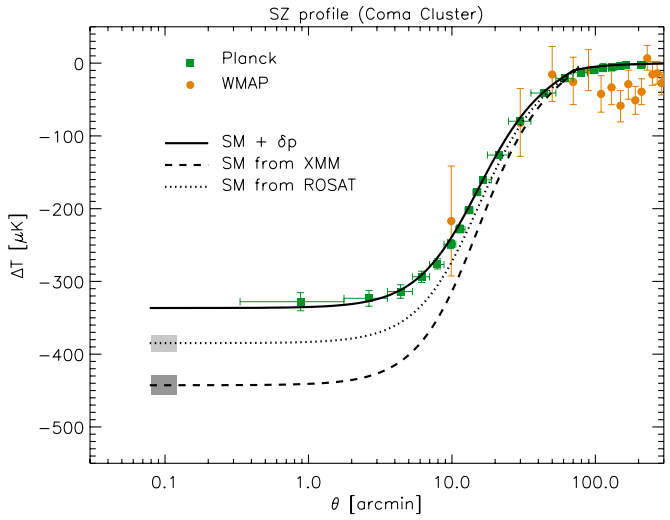

Figure 2. Profile of SZ effect toward the Coma cluster. The green squares refer to the *Planck* data by Ade et al. (2012), and the orange circles to the *WMAP* data by Komatsu et al. (2011). The dashed line illustrates the SM outcome (smoothed on the *Planck* resolution scale) based on the fit to the X-ray data from *XMM-Newton* (see Section 2), with the heavy shaded area representing the associated 2σ uncertainty; the dotted line and light shaded area illustrate the same when based on the fit to the X-ray brightness from *ROSAT* data. The solid line is our outcome when a non-thermal contribution $\delta p/p \approx 20\%$ (or 15%) to the pressure is included in the SM (see Equations 2 and 3).

(A color version of this figure is available in the online journal.)

Such an SZ versus X-ray mismatch goes also beyond the uncertainties affecting the entropy parameters from the X-ray fits (cf. shaded areas in Figures 1 and 2), with effects damped out by the weak dependence on $k(r)$ of the integral term in Equation (2). The mismatch may be marginally alleviated if one relied on the X-ray data from *ROSAT* instead of *XMM-Newton* which, with its higher-resolution instruments, may enhance the clumpiness effects, thus highly biasing the brightness (see Churazov et al. 2012). On the other hand, we recall from Section 1 that an analogous SZ versus X-ray mismatch is obtained with quite different fitting tools by Ade et al. (2012). Thus the tension is *model-independent* and calls for a physical explanation in terms of a pressure contribution adding to the thermal value p.

In this context, the SM formalism is endowed with an extra gear (Cavaliere et al. 2011), i.e., its ability to straightforwardly include in the equilibrium a *non-thermal* component δp to yield the total pressure $p + \delta p$. The result can be simply described in terms of Equation (2), with p and k rescaled to

$$\hat{p} \equiv p\,(1 + \delta p/p), \quad \hat{k} \equiv k\,(1 + \delta p/p). \tag{3}$$

In the above paper we have discussed in one particular instance (focused on turbulence in cluster outskirts) how the pressure $\delta p(r)$ can be physically characterized in terms of a normalization provided by the infall kinetic energy seeping through the virial shocks to drive turbulence, and of a dissipative decay scale.

For Coma a decay scale is not needed, and a nearly uniform $\delta p/p$ applies to a good approximation. Thus the net outcome is to *lower* the normalization applied to the thermal pressure at the virial radius, so that $p_R \propto (1 + \delta p/p)^{-1}$. Resolving the tension between the SZ versus the X-ray data requires $\delta p/p \approx 15\%$ (up to 20% for *XMM-Newton*, which may, however, include a 5% bias due to clumpiness; see above). The outcome is illustrated in Figure 2 by the solid line; we remark that while the SZ profile from the SM has not been derived from a formal fit, it represents well the *Planck* data over their whole radial range. In particular, the *thermal* pressure derived with the SM is now lower by ≈15%, as in fact sensed by the SZ effect.

Note that a uniform $\delta p/p$ implies the density $n \propto (p/k)^{3/5}$ to be closely unaltered, while the temperature normalization is affected as $T_R \propto p_R/n_R \propto (1 + \delta p/p)^{-1}$; this amounts to a minor recalibration in the strength of the virial shocks (see Section 2; also Cavaliere et al. 2009, 2011). The resulting temperature profile stays close to that in Figure 1 (bottom panel) with the thermal component of the central entropy recalibrated to $k_c \approx 470$ from the previous value around 540 keV cm^2.

To sum up, the thermal electron pressure is related to the equilibrium pressure $\hat{p}$ by

$$p_e \approx \frac{0.52\,\hat{p}}{1 + \delta p/p}. \tag{4}$$

With $\delta p/p \approx 15\%$–20%, this boils down to $p_e \approx 0.45$–$0.42\,\hat{p}$, definitely *lower* than the bound $0.5\,p$ pointed out in Section 1. Note that sensible variations in the ICP metallicity $Z \approx 0.4 \pm 0.03$ measured in Coma by Sato et al. (2011) would bias only the electron pressure inferred from the X-ray bremsstrahlung radiation by a few percent, as discussed by Churazov et al. (2012).

4. DISCUSSION AND CONCLUSIONS

Next we discuss the physical nature of such a *non-thermal* pressure contribution δp to the overall equilibrium.

1. Cosmic-ray protons potentially constitute attractive contributors (e.g., Pfrommer et al. 2005) as their energy is long-lived and can be stored within a cluster. However, in Coma their overall energy density has been bounded to be less than a few 10^{-2} of the thermal pressure by radio and γ-ray observations (see Ackermann et al. 2010; Bonafede et al. 2011). On the other hand, cosmic rays may play a role as injectors of secondary electrons, to be subsequently accelerated by turbulence and shocks in the ICP (see Brunetti et al. 2012).
2. Ongoing turbulence originated by recent mergers that drive plasma instabilities in the weakly magnetized ICP constitutes an attractive contributor in view of its direct link to the primary energetics. Such a turbulence has been discussed by many authors as a source of velocity and density fluctuations (see Nagai et al. 2007; Vazza et al. 2010; Iapichino et al. 2011); it is widely held to accelerate with moderate efficiency supra-thermal electrons in the plasma to mildly relativistic energies giving rise to steep distributions (see Schlickeiser et al. 1987; Sarazin & Kempner 2000; Blasi et al. 2007; Brunetti & Lazarian 2011). However, in Coma the density fluctuations caused by ongoing subsonic turbulence have been constrained by Churazov et al. (2012; see their Sections 5.2 and 5.3) to be less than 5% on scales 30–300 kpc. The corresponding indirect estimates of current turbulent velocities $\lesssim$450 km s^{-1} would fall short of providing the additional pressure required to relieve the SZ versus X-ray tension. The actual turbulence velocities will be directly probed with the upcoming *ASTRO-H* mission (http://www.astro-h.isas.jaxa.jp/).
3. Relativistic electrons with Lorentz factors $\gamma \gtrsim 10^3$ in the diffuse magnetic field $B \approx$ a few μG measured in Coma emit the large-scale synchrotron radiation observed at $\nu \gtrsim 30$ MHz in the form of the classic Coma radiohalo; see

Govoni et al. (2001) and Brunetti et al. (2012). Based on the halo shape discussed in Brunetti et al. (2012), the pressures of the magnetic field and of the energetic electrons appear to be effectively coupled to that of the dominant thermal population (see discussions by Brown & Rudnick 2011 and Bonafede et al. 2011). The integrated radio power of several 10^{40} erg s^{-1} implies a relativistic energy density of the order of 10^{-16} erg cm^{-3} (see Giovannini et al. 1993, with parameters updated). Although the corresponding pressure value is substantially smaller than the required $\delta p \approx 0.15\, p \approx$ several 10^{-12} erg cm^{-3}, relativistic electrons can provide interesting candidates if their energy distribution extends steeply toward a lower end $\gamma_1 \lesssim 10^2$.

Such an extension is consistent with the radio spectrum retaining a slope of $\alpha \approx 1.2$ or somewhat steeper, as observed down to frequencies $\nu \approx 31$ MHz (see Henning 1989); the corresponding electron distribution is to rise toward low energies as γ^{-s} with slope $s \equiv 2\alpha + 1 \approx 3.4$. Existing data (cf. Henning 1989) also show that at lower frequencies the radio flux in Coma is still sustained, and may even feature a steeper component, as found in other clusters (see van Weeren et al. 2012); *LOFAR* will soon clear the issue (see http://www.lofar.org/).

The amount of *non-thermal* pressure implied by the above electron population may be estimated as $\delta p \approx \gamma_1\, m_e c^2\, n_{\rm rel}(\gamma_1)/3 \propto \gamma_1^{2-s}$, and refined with the full expressions including mildly relativistic electrons as given by Enßlin & Kaiser (2000, their Appendix A). Using the value 2×10^{40} erg s^{-1} of the radiohalo luminosity at 100 MHz and the profile given by Brunetti et al. (2012), we compute that a non-thermal contribution $\delta p/p \approx 15\%$ would indeed obtain on extending a straight electron distribution down to $\gamma_1 \sim$ a few.

On the other hand, a slope sustained against the fast Coulomb losses (e.g., Sarazin 1999; Petrosian & East 2008) requires that such electrons cannot be drawn from the thermal pool, but rather to have been injected over a few 10^7 yr by the action of mergers, or by AGNs (like the current sources associated with NGC 4869 and NGC 4874), or by cosmic-ray interactions (see Brunetti et al. 2012). These electrons are widely held to be accelerated via turbulence and low-$\mathcal{M}$ shocks, recently driven by mergers deep and energetic but already on the way of dissipating, so as to meet the constraints set by Churazov et al. (2012) and recalled above. We stressed at the end of Section 2 that similar merging events over timescales of Gyr are *independently* required for providing the top level $k_c \approx 500$ keV cm^2 of the central entropy measured in Coma.

Energy distributions steep down to $\gamma_1 \sim$ a few imply a density of $n \sim 10^{-5}$ cm^{-3} in trans-relativistic electrons, and so provide an upper bound for gauging the actual low-γ electron population via the tail of the SZ effect at very high frequencies $\gtrsim$1 THz, and the displacement of the thermal null at 217 GHz; these spectral distortions are illustrated in Figure 3 (see also Rephaeli 1995). Such features in the SZ spectrum are within the reach of sensitive instrumentations like *ALMA* (see http://www.almaobservatory.org/).

In the range $\gamma < 10^2$ the electron distribution will be progressively flattened down by Coulomb interactions over timescales $<10^{-1}$ Gyr. But a "silent pool" of cooling electrons with $\gamma \sim 10^2$ can be replenished and piled up since their lifetimes top at about 1 Gyr. With a cumulative density $n \sim 10^{-7}$ cm^{-3} resulting from many mergers, these electrons can yield a non-thermal contribution $\delta p/p \approx 15\%$. Their synchrotron and relativistic bremsstrahlung radiations would easily escape detection

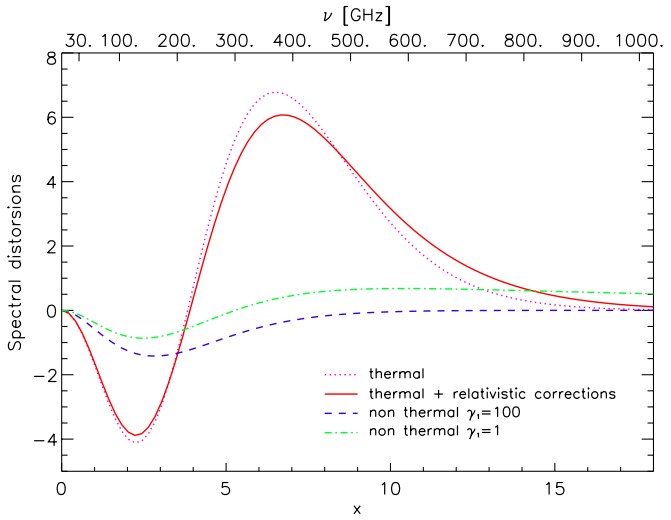

Figure 3. Full spectral distortions of the CMB intensity due to the SZ effect, computed for the Coma cluster. The lower scale represents the quantity $x \equiv h\nu/k_B T_{\rm CMB}$, while the upper scale is labeled with the frequency ν in GHz; note that *Planck* is sensitive to bands in the range $\nu \approx$ 100–857 GHz. The magenta dotted line refers to the thermal SZ effect; the red solid line is the thermal effect with the relativistic corrections for the Coma average temperature $k_B T = 8.2$ keV; the blue dashed line is the non-thermal SZ effect from relativistic electrons down to $\gamma_1 = 10^2$ with density 10^{-7} cm^{-3}, and the green dot-dashed line down to $\gamma_1 = 1$ with density 10^{-5} cm^{-3}. Note the high frequency tail in the latter, and the displacement of the null from the thermal value; see Section 4 for details. A power-law electron energy distribution with spectral index $s = 3.4$ is adopted.

(A color version of this figure is available in the online journal.)

(Sarazin 1999; Sarazin & Kempner 2000), while their collective contribution to pressure is *probed* just by the thermal SZ effect.

In summary, the intriguing physical conditions featured by the inner ICP in the Coma cluster include both a *thermal* and a *non-thermal* component, to be probed via three observational channels across the electromagnetic spectrum: the bremsstrahlung emission in X rays, the thermal and relativistic SZ effects in microwaves, and the diffuse synchrotron radiation in the radio band. On comparing the first two views, we have found a model-independent *tension* between the SZ *Planck* data and the X-ray observations. In fact, a similar mismatch has been also found by Ade et al. (2012) with their empirical fitting formulae, concerning not only spherically averaged profile, but also three out of four angular sectors probed in detail.

On large scales, the tension is difficult to explain in terms of overall asphericities given their limited impact in Coma, as discussed by De Filippis et al. (2005). On small scales, the narrow shock jumps reported in selected sectors by *Planck* (Ade et al. 2012) are diluted by line-of-sight projection and radial averaging. On intermediate scales of the order of several 10^2 kpc, the presence in the ICP of substructures (see Ade et al. 2012) and fluctuations (see Khedekar et al. 2012) may contribute to locally bias the X-ray pressure; however, given the constraints on the density fluctuations in Coma (Churazov et al. 2012), we expect these effects to be limited to about 5%.

We have instead proposed that the SZ versus X-ray tension can be resolved in terms of a physical condition, i.e., a *non-thermal* support $\delta p/p \sim 15\%$–20% yielding a lower effective thermal electron pressure $p_e \approx 0.52\, \hat{p}/(1 + \delta p/p) \approx 0.45$–$0.42\, \hat{p}$; see Equation (4). The spherical SM proceeds to provide a pressure profile that straightforwardly incorporates the *non-thermal* contribution to pressure, and fits in detail the SZ shape while being *consistent* with the resolved X-ray observables

(see Figures 1 and 2). We stress that at variance with the fitting formulae used by Ade et al. (2012), the SM pressure profile features a slow decline for $r \gtrsim 0.3\,R$ in agreement with the *Planck* SZ data. Related pleasing features are also apparent in Figure 1 of Lapi et al. (2012), where the SM is found to perform considerably better than the fitting formulae by Arnaud et al. (2010) in reproducing the stacked SZ profile from several clusters observed with the South Pole Telescope. These successes support our view that the discrepancy between X rays and the SZ effect in Coma is not dominated by specific asymmetries.

Given the current constraints on cosmic-rays and on turbulence (pending direct measurements of the turbulent velocities), we have discussed the additional non-thermal pressure in terms of a mildly relativistic electron population with γ in the range from a few to 10^2. We stress such a component to constitute a natural *byproduct* of the intense merger activity independently required for yielding the very *high* central entropy in the thermal intracluster plasma of the Coma cluster.

We thank the referee for constructive comments. This work is supported in part by ASI, INAF, and MIUR. We thank E. Churazov, J. Gonzalez-Nuevo, P. Mazzotta, and P. Natoli for useful discussions. A.L. thanks SISSA for warm hospitality.

REFERENCES

Ackermann, M., Ajello, M., Allafort, A., et al. 2010, ApJ, 717, L71
Ade, P. A. R., et al. (The *Planck* Collaboration) 2012, A&A, submitted (arXiv:1208.3611)
Arnaud, M., Pratt, G. W., Piffaretti, R., et al. 2010, A&A, 517, 92
Blasi, P., Gabici, S., & Brunetti, G. 2007, IJMPA, 22, 681
Bonafede, A., Govoni, F., Feretti, L., et al. 2011, A&A, 530, A24
Brown, S., & Rudnick, L. 2011, MNRAS, 412, 2
Brunetti, G., Blasi, P., Reimer, O., et al. 2012, MNRAS, 426, 956
Brunetti, G., & Lazarian, A. 2011, MNRAS, 410, 127
Cavagnolo, K. W., Donahue, M., Voit, G. M., & Sun, M. 2009, ApJS, 182, 12
Cavaliere, A., & Fusco-Femiano, R. 1976, A&A, 49, 137
Cavaliere, A., Lapi, A., & Fusco-Femiano, R. 2011, ApJ, 742, 19
Cavaliere, A., Lapi, A., & Fusco-Femiano, R. 2009, ApJ, 698, 580
Churazov, E., Vikhlinin, A., Zhuravleva, I., et al. 2012, MNRAS, 421, 1123
De Filippis, E., Sereno, M., Bautz, M. W., & Longo, G. 2005, ApJ, 625, 108
Enßlin, T. A., & Kaiser, C. R. 2000, A&A, 360, 417
Fabian, A. C. 2012, ARA&A, 50, 455
Fusco-Femiano, R., Cavaliere, A., & Lapi, A. 2009, ApJ, 705, 1019
Giovannini, G., Feretti, L., Venturi, T., Kim, K.-T., & Kronberg, P. P. 1993, ApJ, 406, 399
Govoni, F., Enßlin, T. A., Feretti, L., & Giovannini, G. 2001, A&A, 369, 441
Henning, P. A. 1989, AJ, 97, 1561
Iapichino, L., Schmidt, W., Niemeyer, J. C., & Merklein, J. 2011, MNRAS, 414, 2297
Khedekar, S., Churazov, E., Kravtsov, A., et al. 2012, MNRAS, submitted (arXiv:1211.3358)
Komatsu, E., Smith, K. M., Dunkley, J., et al. 2011, ApJS, 192, 18
Lapi, A., & Cavaliere, A. 2009, ApJ, 695, L125
Lapi, A., Cavaliere, A., & De Zotti, G. 2003, ApJ, 597, L93
Lapi, A., Cavaliere, A., & Fusco-Femiano, R. 2012, ApJL, 745, 15
Lapi, A., Cavaliere, A., & Menci, N. 2005, ApJ, 619, 60
Markevitch, M. 2012, in Proc. of the 12th Marcel Grossmann Meeting on General Relativity, ed. T. Damour, R. T. Jantzen, & R. Ruffini (Singapore: World Scientific), 397
Markevitch, M., & Vikhlinin, A. 2007, PhR, 443, 1
McCarthy, I. G., Bower, R. G., Balogh, M. L., et al. 2007, MNRAS, 376, 497
Mohr, J. J., Mathiesen, B., & Evrard, A. E. 1999, ApJ, 517, 627
Molendi, S., & Pizzolato, F. 2001, ApJ, 560, 194
Nagai, D., Kravtsov, A. V., & Vikhlinin, A. 2007, ApJ, 668, 1
Petrosian, V., & East, W. E. 2008, ApJ, 682, 175
Pfrommer, C., Enßlin, T. A., & Sarazin, C. L. 2005, A&A, 430, 799
Pratt, G. W., Arnaud, M., Piffaretti, R., et al. 2010, A&A, 511, A85
Rephaeli, Y. 1995, ARA&A, 33, 541
Sarazin, C. G. 1999, ApJ, 520, 529
Sarazin, C. G., & Kempner, J. C. 2000, ApJ, 533, 73
Sato, T., Matsushita, K., Ota, N., et al. 2011, PASJ, 63, 991
Schlickeiser, R., Sievers, A., & Thiemann, H. 1987, A&A, 182, 21
Snowden, S. L., Mushotzky, R. F., Kuntz, K. D., & Davis, D. S. 2008, A&A, 478, 615
Sunyaev, R. A., & Zeldovich, Ya. B. 1980, ARA&A, 18, 537
Tozzi, P., & Norman, C. 2001, ApJ, 546, 63
van Weeren, R. J., Röttgering, H. J. A., Rafferty, D. A., et al. 2012, A&A, 543, A43
Vazza, F., Brunetti, G., Gheller, C., & Brunino, R. 2010, NewA, 15, 695
Vikhlinin, A., Kravtsov, A., Forman, W., et al. 2006, ApJ, 640, 691
Voit, G. M. 2005, RvMP, 77, 207
Walker, S., Fabian, A., Sanders, J., & George, M. 2012, MNRAS, 427, L45
Wik, D. R., Sarazin, C. L., Finoguenov, A., et al. 2009, ApJ, 696, 1700